

Achievement of FCC specification in critical current density for Nb₃Sn superconductors with artificial pinning centers

X Xu¹, X Peng², J Rochester³, M Sumption³ and M Tomsic²

¹Fermi National Accelerator Laboratory, Batavia, IL 60510, U.S.A

²Hyper Tech Research Incorporated, 539 Industrial Mile Road, Columbus, OH 43228, U.S.A

³Department of MSE, the Ohio State University, Columbus, OH 43210, U.S.A

E-mail: xxu@fnal.gov

Abstract

In this letter we demonstrate achievement of record non-Cu critical current density ($J_{c,non-Cu}$) in ternary, multifilamentary Nb₃Sn conductors by the introduction of artificial pinning centers (APC). In the past two years, we have made great progress in the development of APC Nb₃Sn wires. Recent resistivity vs magnetic field measurements confirmed the high upper critical field (B_{c2}) of ternary APC wires, which at 4.2 K was ~28 T, about 1-2 T higher than present state-of-the-art conductors. In addition to high B_{c2} , it was found that APC wires have noticeably higher Sn content in the Nb₃Sn layers as compared to standard wires. The $J_{c,non-Cu}$ values of the most-recent APC wires have met the $J_{c,non-Cu}-B$ specification required by the Future Circular Collider (FCC), with the best heat treatment leading to a $J_{c,nonCu}$ 29% higher than the FCC specification at 21 T. Microscopy analysis shows that the APC wires still have overly high residual Nb fractions due to too low of a Sn/Nb ratio, indicating that there is still great potential for further $J_{c,non-Cu}$ improvement. The development of APC wires is ongoing; this letter details some of the steps forward in the optimization and lays out a roadmap to push the APC wires towards practical, magnet-grade conductors.

Keywords: Nb₃Sn Superconductor, Artificial pinning center, B_{c2} , J_c .

1. Introduction

The proposed High-Energy Large Hadron Collider (HE-LHC) upgrade as well as Future Circular Collider (FCC) aims to push the energy frontier for high energy physics, and both require thousands of 16 T dipoles based on Nb₃Sn superconductors [1]. Design studies of such magnets have been pursued in earnest for a few years using Nb₃Sn conductor specifications that include a non-Cu critical current density versus field ($J_{c,non-Cu}-B$) curve which at 4.2 K and 16 T is 1500 A/mm² at a minimum [2,3]. Conductor $J_{c,non-Cu}$ is a critical factor for such large machines because building 16 T magnets with conductors of lower $J_{c,non-Cu}$ would require a larger coil size and thus significantly increase the overall project cost. The rod-restack-process (RRP[®]) wires, which are the present state-of-the-art Nb₃Sn conductors, meet the $J_{c,non-Cu}$ specification required by the High-Luminosity LHC (HL-LHC) upgrade with ~3% margin [4]. However, the FCC $J_{c,non-Cu}$ specification is 50% higher than the HL-LHC specification [1-3], which means that a ~45% improvement is still needed for state-of-the-art Nb₃Sn wires to fulfill the FCC requirement with a reasonable conductor acceptance fraction. This is a huge challenge considering that the record $J_{c,non-Cu}$ of Nb₃Sn wires has been at a plateau since the early 2000s [5] despite extensive efforts to break this barrier [6].

Introduction of artificial pinning centers (APC) to enhance flux pinning and thus J_c has long been a “holy grail” in the Nb₃Sn area. Significant efforts had been made using various techniques since the 1980s but none succeeded in producing superior J_c in wires [7-12] except proton or neutron irradiation [13,14] which is not practical for magnets. This was finally realized in 2014 [15] via the internal oxidation method, a technology that was used in Nb₃Sn tapes in the 1960s [16] but had been believed ineffective in Nb₃Sn wires after some unsuccessful attempts in the

2000s (e.g., [10,11]). About a decade later we revisited this idea and were able to find out the essentials for it to work in Nb₃Sn wires [15]. We first demonstrated using binary monofilaments the effects of this technique (e.g., significantly refined grain size, doubled layer J_c at 12 T despite low irreversibility field – B_{irr} , shift of pinning force curve peak from $0.2B_{irr}$ to $0.34B_{irr}$, etc.) [15,17], and subsequently proposed applying it in the powder-in-tube (PIT) design in order to make multifilamentary wires [17,18]. Later binary multi-filamentary wires were fabricated by SupraMagnetics Inc. [19] and Hyper Tech Research Inc. [20], which confirmed the monofilament results. On the other hand, the low B_{irr} seen in these binary APC wires [17,19,20] showed the need for ternary dopants. From 2017 several groups started to study the effect of ternary doping to APC wires, including Florida State University (FSU) [21] and University of Geneva [22], as well as a collaboration between Hyper Tech, Fermilab, and the Ohio State University (OSU) that began in earnest to develop ternary multifilamentary APC-PIT wires. As a surprising side result, FSU found in monofilaments grain refinement via Hf doping without internal oxidation, which also looks to be a promising method to improve Nb₃Sn J_c [21].

The transport resistance vs field (R - B) and voltage vs current (V - I) tests up to 31 T in late 2018 [23] on the first set of ternary multifilamentary APC wires developed jointly by Hyper Tech, Fermilab, and OSU clearly demonstrated that the low B_{irr} issue seen in binary APC wires had been solved by addition of Ta dopant, which was also seen in the monofilaments in [21] and [22]. In fact, the B_{irr} and B_{c2} values (4.2 K) of the APC wire with 1wt.% Zr (T3882-0.84mm-675°C/300h, denoted “APC-B” in [23]) were 26.8 and 27.6 T, respectively, ~2 T higher than the reference RRP[®] wire that is used for the HL-LHC. The measured $J_{c,non-Cu}$ (4.2 K, 16 T) of T3882-0.84mm-675°C/300h had reached a similar level to that of the reference RRP[®] wire. Scanning electron microscopy (SEM) analysis showed that the average fine-grain (FG) Nb₃Sn

fraction in the filaments of T3882-0.84mm-675°C/300h was only 22%, while the residual Nb fraction was as high as 45%. Indeed, the FG Nb₃Sn layer J_c of T3882-0.84mm-675°C/300h was 2.5 times higher than that of the reference RRP[®] wire at 4.2 K, 16 T (4710 vs 1870 A/mm²) [23]. This made it clear that there was still huge potential for further improvement of $J_{c,non-Cu}$ via precursor ratio optimization, which could allow more FG formation.

A second set of ternary APC wires had been developed, guided by the analysis on the first set of wires, and were tested in early 2019. The results, reported here, not only confirm the high B_{irr} and B_{c2} of ternary APC wires, but also demonstrate $J_{c,non-Cu}$ which has achieved (or surpassed) the FCC specification at high fields.

2. Experimental

2.1. Samples

The APC wire used here, T3912, is based on a 48/61-filament design (i.e., 48 Nb₃Sn and 13 Cu filaments) with a Cu/non-Cu ratio of 1.3, fabricated at Hyper Tech using a Nb-1wt.%Zr-7.5wt.%Ta tube and a mixture of Cu, Sn, and SnO₂ powders. Compared with T3882 [23], the Sn/Nb and SnO₂/Nb ratios were increased in T3912. Most of the filaments of T3912 had sufficient oxygen. The wire was fabricated using a billet with a starting diameter of 19 mm, which was drawn to final wire diameters of 0.5, 0.71, and 0.84 mm, resulting in a total length of ~200 meters. Two commercial, state-of-the-art, Nb₃Sn wires were tested together with the T3912 samples as references: one was a Ti-doped RRP[®] wire (billet number 00076) with 0.85mm diameter and 108/127 subelements, and the other was a standard PIT wire (billet number 31284) with 0.78mm diameter and 192/217 filaments; both wires were manufactured by Bruker EST and used for HL-LHC.

All wires were heat treated under vacuum. The APC wires were reacted at 675°C, 685°C, and 700°C for various durations (specified below), all with a ramp rate of 30°C/h without intermediate steps. The RRP[®] wire used the HL-LHC HT protocol: 210°C/48h + 400°C/48h + 665°C/75h [4]. The standard PIT wire used a two-stage HT 630°C/100h + 640°C/50h in order to maximize its $J_{c,non-Cu}$ while maintaining high residual resistivity ratio (RRR) [24].

2.2. Measurements

Two types of transport tests were performed on these wires at the National High Magnetic Field Laboratory (NHMFL): (1) *R-B* measurements using a sensing current of 31.6 mA, allowing determinations of B_{c2} and B_{irr} , (2) *V-I* measurements at various fields, giving critical current (I_c) values. All tests were at 4.2 K in a 31T magnet with fields perpendicular to wire axes. Great care was taken to ensure that each sample was centered within the magnet. The *R-B* tests were performed on samples 15mm in length with a voltage tap spacing of 5 mm. Since five samples could be mounted together in the holder for each run, we always included one reference wire in order to give a double check on the results. The *V-I* measurements used the I_c transport test system from the Applied Superconductivity Center (ASC) at the NHMFL (including the I_c rig, sample holders, data acquisition system, testing program, etc.), and were performed on straight samples 35mm in length with a voltage tap separation of 6 mm. A criterion of 0.1 $\mu\text{V/cm}$ was used to determine the I_c values. The compositions of the Nb₃Sn layers were measured using energy-dispersive spectroscopy (EDS): 25kV voltage was used, with a collection rate above 40000 counts per second, and for each spot data were collected for 30 seconds.

3. Measurement results

The R - B curve of T3912 (0.84mm diameter given a HT of 675°C/384h) is shown in Figure 1, along with those of T3882-0.84mm-675°C/300h [23] as well as the reference wires. Below we take the fields at 10% and 90% of the normal state resistances as B_{irr} and B_{c2} , respectively.

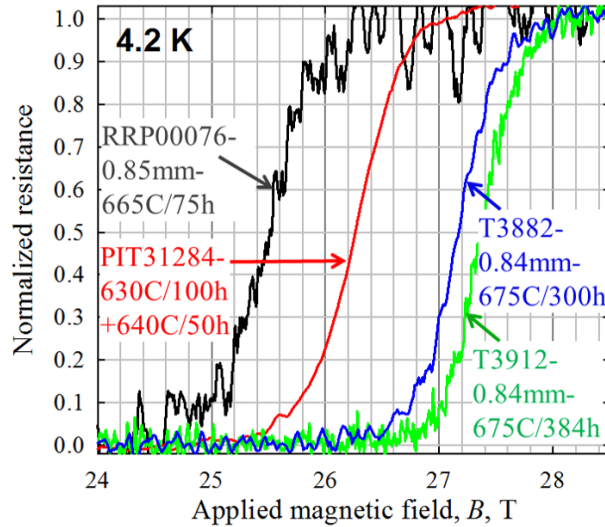


Figure 1. The 4.2K R - B curves of the reference wires as well as T3882-0.84mm-675°C/300h [23] and T3912-0.84mm-675°C/384h.

The B_{irr} and B_{c2} of the RRP[®] wire were ~25 and ~26 T, respectively, which are typical for RRP[®] wires reacted at 665°C. The standard PIT wire had B_{irr} and B_{c2} of 25.8 and 26.7 T, respectively, which are similar to what Godeke measured for PIT wires reacted at 675°C [25] and are nearly 1T higher than those of the RRP[®] wire. The 4.2K B_{irr} and B_{c2} of T3912-0.84mm-675°C/384h were 27 and 27.8 T, respectively, over 1T higher than those of the standard PIT wire. These results confirm our previous measurements in late 2018 [23] showing that the ternary APC wires have higher B_{irr} and B_{c2} than the standard PIT and RRP[®] conductors.

The measured $J_{c,non-Cu}$ values of the reference wires and T3882-0.84mm-675°C/300h [23] as well as T3912 given various heat treatments are shown in Figure 2, along with the FCC $J_{c,non-Cu}$

B specification curve that is generated using the equations and parameters given in [3]. Here it is worth mentioning that design of a magnet with 16T bore field (which leads to a slightly higher peak field on the conductors [3]) in fact requires the use of $J_{c,non-Cu}$ at a higher field (e.g., ~19 T for a 14% margin [3] along the peak field load line) – indeed, a calculation of conductor temperature margin shows that the 19T $J_{c,non-Cu}$ is more relevant than the 16T $J_{c,non-Cu}$; therefore, the 19T $J_{c,non-Cu}$ values will also be reported below. The 16T $J_{c,non-Cu}$ values of the RRP[®] and PIT wires were 1090 and 1005 A/mm², and the 19T values were 395 and 410 A/mm², respectively. These are not the highest values for top-performing RRP[®] and PIT wires (which are ~1300 A/mm² at 16 T [2]), but are in their typical $J_{c,non-Cu}$ spectrums. Despite lower $J_{c,non-Cu}$ at low fields, PIT wires outperform RRP[®] at high fields (19 T and above) due to higher B_{irr} , which has also been seen previously [2]. Because the I_c values of the APC wires with 0.84mm diameter could not be obtained at low fields due to quenching during the $V-I$ tests (which could be due to large subelement size D_s and a bit too long reaction times), the $J_{c,non-Cu}-B$ data are fitted with a commonly-used two-component pinning force model, which has been shown by a number of studies to work well for both standard and APC wires [9,19,23]. As can be seen in Figure 2, the fittings to the data are good. The $J_{c,non-Cu}$ of T3912 at 0.71mm diameter (with D_s of 70 μ m) after a HT of 700°C/71h was 3% lower than the FCC specification at 16 T, but surpassed the latter at 19 T and above. The RRR of this wire was 85 – improvement of RRR requires further improvement of wire quality as well as HT optimization studies to prevent too long reaction time. With the same HT temperature of 700°C, an increase of the wire diameter to 0.84 mm (with D_s of 83 μ m) led to only slightly higher $J_{c,non-Cu}$ (by <5%). On the other hand, lower HT temperatures led to substantially higher $J_{c,non-Cu}$: e.g., reducing HT to 685°C increased the $J_{c,non-Cu}$ to 730 A/mm² at 19 T (i.e., 13% higher than the FCC specification) and extrapolated 1600 A/mm² at 16 T. Further

reducing HT to 675°C led to even higher $J_{c,non-Cu}$: e.g., 380 A/mm² at 21 T (i.e., 29% higher than the FCC specification), and extrapolated values of 780 A/mm² at 19 T and 1740 A/mm² at 16 T, the latter being 16% higher than the FCC specification and ~30% higher than the RRP[®] record.

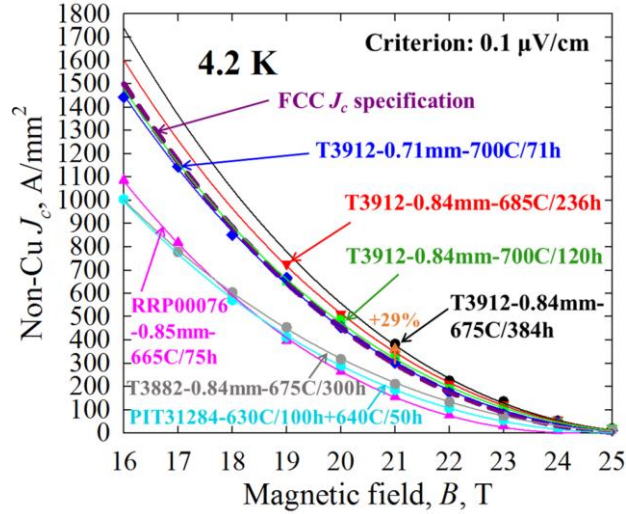


Figure 2. Non-Cu J_c s of the reference and the APC wires, as well as the FCC $J_{c,non-Cu-B}$ specification.

4. Discussions

In addition to the high B_{irr} and B_{c2} , we found that APC wires also had higher Sn content in the FG layers as compared to that in conventional wires. The Sn concentrations in Nb₃Sn of T3912 as well as those of several other wires (all with 48/61 design) with different combinations of Zr, Ta, and O, as shown in Table 1, were measured and are shown in Figure 3. For all of the samples, the first EDS spots were in the coarse-grain (CG) Nb₃Sn regions (which are known to have Sn content around 25 at.% [26]), and the last spots were close to the FG/Nb interfaces, while all the other spots were in the FG layers. In Nb₃Sn wires, only the FG layers can carry supercurrents, while the CG cannot. It can be seen that T3736, T3814, and T3843 generally had

Sn concentrations in FG between 22.5 and 24 at.%, which are typical for standard Nb₃Sn wires [26]. On the other hand, T3739 and T3912 had Sn concentrations in FG between 24 and 25 at.%, close to stoichiometry. By comparing these wires, it can be clearly seen that only the internally oxidized samples (Zr+O) had the highest Sn content in FG. To verify the Sn content results, several APC and standard PIT and tube type wires given the same HT (675°C/120h) were sent as blind samples to Ian Pong at Lawrence Berkley National Laboratory (LBNL) for EDS verification measurements. The results of detailed line-scan measurements by Pong confirmed that the Sn concentrations of the APC wires were 1-1.5 at.% higher than those of standard wires [27]. The enhanced Sn content in the APC wires is possibly due to the reduced reaction rate at the Nb₃Sn/Nb interface [17], which, according to a diffusion reaction theory for Nb₃Sn composition [6,28], benefits the Sn content of a Nb₃Sn layer.

Table 1. Summary of the wires for EDS studies

Wire	Diameter, mm	Tube	Core	Chemistry
T3736	1.0	Nb-7.5wt.%Ta	Cu-clad Sn rod	With Ta, but no Zr or O
T3739	0.84	Nb-1wt.%Zr	Mixture of Cu, Sn, and SnO ₂ powders	With Zr and O, but no Ta
T3814	0.84	Nb-1wt.%Zr-7.5wt.%Ta	Mixture of Cu and Sn powders	With Zr and Ta, but no O
T3843	0.84	Nb-7.5wt.%Ta	Mixture of Cu, Sn, and SnO ₂ powders	With Ta and O, but no Zr

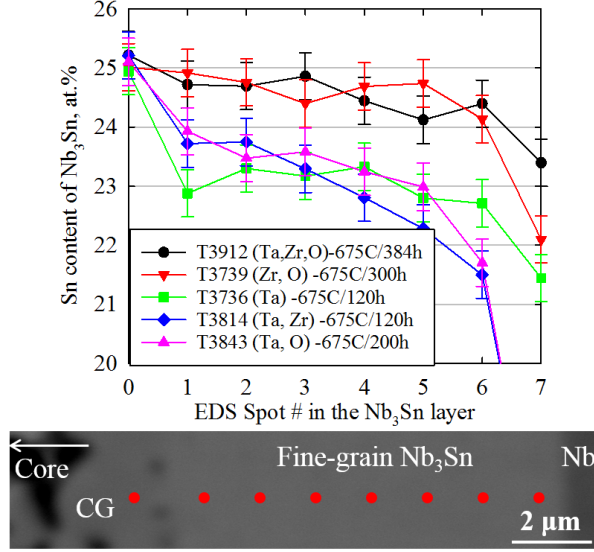


Figure 3. Sn concentrations in Nb₃Sn layers of the selected wires and a schematic showing the EDS spots.

The B_{irr} and B_{c2} of Nb₃Sn depend on both Sn content and doping. Ti and Ta dopants may have different influences on B_{c2} and also on Sn content due to possible different site occupancy, which was studied in [29] and recently [30]. Here we compare standard PIT and our APC wires, all based on Ta doping. It is well known (e.g., [6,26,29]) that for ternary Nb₃Sn, B_{c2} increases with Sn content. Therefore, the higher Sn content in FG Nb₃Sn of the ternary APC wires could be why they have higher B_{irr} and B_{c2} than standard PIT wires.

SEM images of cross sections of T3912-0.71mm-700°C/71h and T3912-0.84mm-675°C/384h are shown in Figure 4. From these images the average area fractions of FG, residual Nb, and CG in filaments of both wires were calculated and are shown in Table 2, along with those of T3882-0.84mm-675°C/300h [23] as well as standard PIT conductors. From Table 2, the FG fractions of both T3912 wires are nearly 50% higher than that of the T3882-0.84mm-675°C/300h: this is the primary reason for the much higher $J_{c,non-Cu}$ of T3912 in comparison to

T3882; a secondary reason is an improvement of wire uniformity (T3882 had a number of filaments with insufficient oxygen [23]). Since T3912-0.84mm-675°C/384h has lower FG fractions than T3912-0.71mm-700°C/71h, its higher $J_{c,non-Cu}$ is most likely due to higher flux pinning as a result of the lower HT temperature. The residual Nb fractions of both T3912 wires (34%) are still much higher than those of standard PIT wires (typically 25% or below [24]). A closer analysis of the recipe of T3912 reveals that this is because it has too low of a Sn/Nb ratio. This means that the APC wires still have the potential to form more FG by converting more Nb by properly tweaking the recipe design, which is expected to lead to higher $J_{c,non-Cu}$.

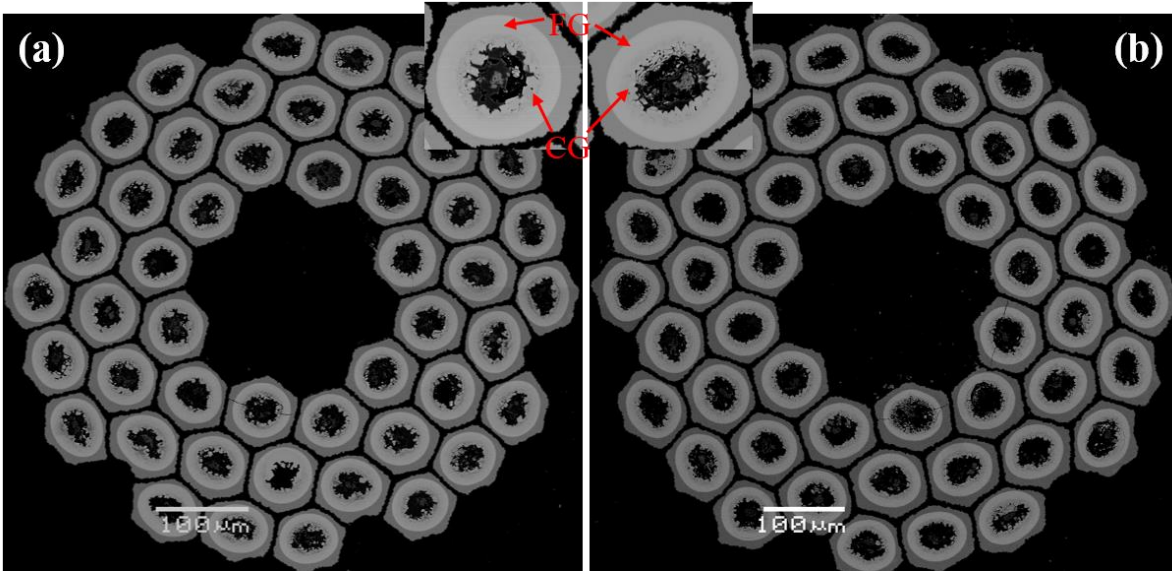


Figure 4. SEM images of cross sections for (a) T3912-0.71mm-700°C/71h, and (b) T3912-0.84mm-675°C/384h.

Table 2. Area fractions in filaments of T3882 and T3912 wires as well as standard PIT wires

Areas	T3882-0.84mm-675°C/300h [23]	T3912-0.71mm-700°C/71h	T3912-0.84mm-675°C/384h	Standard PIT [24]
Fine-grain A15	22%	33%	31%	40%
Residual Nb	45%	34%	34%	25%
Coarse-grain A15	13%	14%	16%	13%

Despite achievement of the FCC $J_{c,non-Cu}$ specification, there is still much work to be done. First, it is necessary to continue to optimize the wire recipe, which on one hand may lead to better Nb/Sn ratio for a fuller reaction and thus higher $J_{c,non-Cu}$, and on the other hand will also likely further improve wire quality and thus RRR, considering that recipe optimization has been the primary contributor to the improvement of APC wire quality (e.g., filament shape) in the past two years. Second, it is important to continue to optimize the HT of APC wires because a lower HT temperature benefits $J_{c,non-Cu}$ and proper reaction times are required to retain high RRR. Third, exploration of some wire design variants that have been demonstrated in standard PIT wires could be very helpful in improving performance of APC wires, such as the use of round filaments instead of the present hexagonal ones (this improves $J_{c,non-Cu}$ because it allows more Nb to be converted into Nb_3Sn without poisoning the RRR) and the use of a bundle barrier (which is effective in preserving high RRR) [31]. Next, it is necessary to continue the fabrication and optimization of 217-filament wires, which are important for reduction of D_s and thus improvement of conductor stability. We have fabricated a wire with 217 filaments using a Nb-0.6wt.%Zr-7.5wt.%Ta tube, which was drawn to 0.71mm diameter (with D_s of 35 μm) without wire breakage. A next logical step would be fabrication of wires with 217 filaments using Nb-1wt.%Zr-7.5wt.%Ta tubes for higher $J_{c,non-Cu}$. Here it is worth mentioning that APC wires demonstrate good drawability: all the APC wires of the past 23 billets (including 13 using Nb-0.6wt.%Zr-7.5wt.%Ta tubes and 10 using Nb-1wt.%Zr-7.5wt.%Ta tubes) were drawn to 0.5-0.84mm diameters in single pieces without any wire breakage. In parallel with the above research and development tasks, there are other tasks which are needed in order to push APC wires towards practical, magnet-grade conductors, such as process improvement and increased

billet size, etc., as well as evaluation of electro-mechanical properties (e.g., uniaxial tensile and transverse pressure tests), which are important for magnet applications.

5. Conclusions

Our results reported here on multifilamentary APC Nb₃Sn conductors confirm the high B_{irr} and B_{c2} of ternary, internal oxidation route APC wires (27-28 T at 4.2 K), which are 1-2 T higher than RRP[®] and standard PIT wires. This is because APC wires have significantly higher Sn content in the Nb₃Sn layer as compared to those without internal oxidation. The $J_{c,non-Cu}$ values of these recent APC wires have achieved the FCC $J_{c,non-Cu}-B$ specification, and a HT at 675°C led to a $J_{c,non-Cu}$ 29% higher than the FCC specification at 21 T. Analysis of SEM images showed that the FG Nb₃Sn fractions have increased dramatically, but are still below what we estimate is possible for properly optimized chemistries. Finally, some work remains to be done in order to further improve performance of APC wires and push them towards practical conductors, and we see a potentially viable path to make magnet-grade, long-length APC Nb₃Sn conductors.

Acknowledgements

This work is supported by the Laboratory Directed Research and Development (LDRD) program of Fermilab and Hyper Tech SBIR DE-SC0013849 and DE-SC0017755 by US Department of Energy. Some tests were performed at the NHMFL, which is supported by National Science Foundation Cooperative Agreement No. DMR-1644779 and the State of Florida. The measurements at the NHMFL were greatly helped by Jan Jaroszynski, Griffin Bradford, and Yavuz Oz. We are grateful to ASC of the NHMFL for letting us use the I_c

transport test system. We thank Ian Pong from LBNL for supplying the RRP[®] and PIT wires that are used as references in this work, and for the independent EDS studies that confirmed our results. This work is performed under the auspices of U.S. Magnet Development Program.

References

- [1]. Benedikt M and Zimmermann F 2016 Status of the future circular collider study *CERN-ACC-2016-0331*
- [2]. Ballarino A and Bottura L 2015 Targets for R&D on Nb₃Sn Conductor for High Energy Physics *IEEE Trans. Appl. Supercond.* **25** 6000906
- [3]. Tommasini D and Toral F 2016 Overview of magnet design options *CERN Report EuroCirCol-P1-WP5* pp 4-6
- [4]. Cooley L D, Ghosh A K, Dietderich D R and Pong I 2017 Conductor Specification and Validation for High-Luminosity LHC Quadrupole Magnets *IEEE Trans. Appl. Supercond.* **27** 6000505
- [5]. Parrell J A, Zhang Y Z, Field M B, Cisek P and Hong S 2003 High field Nb₃Sn conductor development at Oxford Superconducting Technology *IEEE Trans. Appl. Supercond.* **13** 3470-3
- [6]. Xu X 2017 A review and prospects for Nb₃Sn superconductor development *Supercond. Sci. Technol.* **30** 093001
- [7]. Flukiger R, Specking W, Klemm M and Gauss S 1989 Composite core Nb₃Sn wires: preparation and characterization *IEEE Trans. Magn.* **25** 2192-9
- [8]. Zhou R, Hong S, Marancik W and Kear B 1993 Artificial flux pinning in Nb and Nb₃Sn superconductors *IEEE Trans. Appl. Supercond.* **3** 986-9
- [9]. Rodrigues D, Da Silva L B S, Rodrigues C A, Oliveira N F and Bormio-Nunes C 2011 Optimization of Heat Treatment Profiles Applied to Nanometric-Scale Nb₃Sn Wires With Cu-Sn Artificial Pinning Centers *IEEE Trans. Appl. Supercon.* **21** 3150-3
- [10]. Zeitlin B A, Marte J, Ellis D, Benz M and Gregory E 2003 Some Effects of the Addition of 1 at% Zr to Nb on the Properties and Ease of Manufacture of Internal-Tin Nb₃Sn *Adv. Cryog. Eng.* **50B** 895-902
- [11]. Zeitlin B A, Gregory E, Marte J, Benz M, Pyon T, Scanlan R and Dietderich D 2005 Results on Mono Element Internal Tin Nb₃Sn Conductors (MEIT) with Nb_{7.5}Ta and Nb(1Zr+O_x) Filaments *IEEE Trans. Appl. Supercond.* **15** 3393-6
- [12]. Motowidlo L R, Lee P J and Larbalestier D C 2009 The Effect of Second Phase Additions on the Microstructure and Bulk Pinning Force in Nb₃Sn PIT Wire *IEEE Trans. Appl. Supercond.* **19** 2568-72
- [13]. Baumgartner T, Eisterer M, Weber H W, Flükiger R, Scheuerlein C and Bottura L 2015 Performance Boost in Industrial Multifilamentary Nb₃Sn Wires due to Radiation Induced Pinning Centers *Sci. Rep.* **5** 10236
- [14]. Spina T, Scheuerlein C, Richter D, Bordini B, Bottura L, Ballarino and Flükiger R 2015 Artificial Pinning in Nb₃Sn Wires *IEEE Trans. Appl. Supercond.* **27** 8001205

- [15]. Xu X, Sumption M D, Peng X and Collings E W 2014 Refinement of Nb₃Sn grain size by the generation of ZrO₂ precipitates in Nb₃Sn wires *Appl. Phys. Lett.* **104** 082602
- [16]. Benz M G 1968 The superconducting performance of diffusion processed Nb₃Sn doped with ZrO₂ particles *Trans. of Met. Soc. of AIME* **242** 1067-70
- [17]. Xu X, Sumption M D and Peng X 2015 Internally Oxidized Nb₃Sn Superconductor with Very Fine Grain Size and High Critical Current Density *Adv. Mater.* **27** 1346-50
- [18]. Xu X, Sumption M D and Peng X 2018 Superconducting wires and methods of making thereof *U.S. Patent 9916919*, filed date: Feb. 18, 2015
- [19]. Motowidlo L, Lee P J, Tarantini C, Balachandran S, Ghosh A and Larbalestier D C 2017 An intermetallic powder-in-tube approach to increased flux-pinning in Nb₃Sn by internal oxidation of Zr *Supercond. Sci. Technol.* **31** 014002
- [20]. Xu X, Peng X, Sumption M D and Collings E W 2017 Recent Progress in Application of Internal Oxidation Technique in Nb₃Sn Strands *IEEE Trans. Appl. Supercond.* **27** 6000105
- [21]. Balachandran S, Tarantini C, Lee P J, Kametani F, Su Y, Walker B, Starch W L and Larbalestier D C 2019 Beneficial influence of Hf and Zr additions to Nb_{4at.%Ta} on the vortex pinning of Nb₃Sn with and without an O Source *Supercond. Sci. Technol.* **32** 044006
- [22]. Buta F, Bonura M, Matera D, Ballarino A, Hopkins S, Bordini B and Senatore C 2018 Properties and microstructure of binary and ternary Nb₃Sn superconductors with internally oxidized ZrO₂ nanoparticles *Applied Supercond. Conf.* 1MPo2A-06
- [23]. Xu X, Rochester J, Peng X, Sumption M D and Tomsic M 2019 Ternary Nb₃Sn conductors with artificial pinning centers and high upper critical fields *Supercond. Sci. Technol.* **32** 02LT01
- [24]. Segal C, Tarantini C, Lee P J and Larbalestier D C 2017 Improvement of small to large grain A15 ratio in Nb₃Sn PIT wires by inverted multistage heat treatments *IOP Conf. Ser. Mater. Sci. Eng.* **279** 012019
- [25]. Godeke A, Jewell M, Fischer C, Squitieri A, Lee P and Larbalestier D 2005 The upper critical field of filamentary Nb₃Sn conductors *J. Appl. Phys.* **97** 093909
- [26]. Hawes C D, Lee P J and Larbalestier D C 2006 Superconductor Science and Technology Measurements of the microstructural, microchemical and transition temperature gradients of A15 layers in a high-performance Nb₃Sn powder-in-tube superconducting strand *Supercond. Sci. Technol.* **19** S27-37
- [27]. Pong I, unpublished data
- [28]. Xu X and Sumption M 2016 A model for the compositions of non-stoichiometric intermediate phases formed by diffusion reactions, and its application to Nb₃Sn superconductors *Sci. Rep.* **6** 19096
- [29]. Flukiger R, Uglietti D, Senatore C and Buta F 2008 Microstructure, composition and critical current density of superconducting Nb₃Sn wires *Cryogenics* **48** 293-307
- [30]. Heald S M, Tarantini C, Lee P J, Brown M D, Sung Z, Ghosh A K and Larbalestier D C 2018 Evidence from EXAFS for Different Ta/Ti Site Occupancy in High Critical Current Density Nb₃Sn Superconductor Wires *Sci. Rep.* **8** 4798
- [31]. Bordini B, Ballarino A, Macchini M, Richter D, Sailer B, Thoener M and Schlenga K 2017 The Bundle-Barrier PIT Wire Developed for the HiLumi LHC Project *IEEE Trans. Appl. Supercond.* **27** 6000706